

The feasibility of generating low frequency volcano seismicity by flow through a deformable channel

A. C. Rust¹

University of Bristol, Wills Memorial Building, Bristol BS8 1RJ, UK

Alison.Rust@bristol.ac.uk

N. J. Balmforth²

Department of Mathematics &

Department of Earth & Ocean Sciences, University of British Columbia, Vancouver, Canada

& S. Mandre³

Division of Engineering and Applied Sciences, Harvard University, Boston, U.S.A.

December 4, 2006

Abstract

Oscillations generated by flow of magmatic or hydrothermal fluids through tabular channels in elastic rocks are a possible source of low frequency seismicity. We assess the conditions required to generate oscillations of $\sim 1\text{Hz}$ *via* hydrodynamic flow instabilities, flow-destabilized standing waves set up on the channel walls, and unstable normal modes ringing in an adjacent fluid reservoir. Flow destabilized modes offer the most plausible explanation, but there are limitations on what kind of standing waves comprises them.

Introduction

Tremor, as well as shorter duration long-period (LP) seismic events, are important indicators of unrest at volcanoes, and as such are used to evaluate eruption hazards and to invert for the geometry and nature of fluids in volcanoes (Chouet 1996, 2003; McNutt 2005). It is widely accepted that this low-frequency volcano seismicity emanates from fluid channels encased in rock, such as fluid-filled hydrofractures, dykes and cylindrical conduits. However, the precise mechanism responsible for generating those signals is still under debate, particularly for harmonic tremor.

One prominent explanation for these harmonic signals is that they stem from the resonant excitation of standing waves in the fluid channel. Individually, both the fluid and solid support their own kind of waves (elastic and acoustic, respectively). But these wave types propagate relatively quickly, and if the standing waves have either elastic or acoustic origin, then the resonating body may be excessively large to match typical tremor periods. However, the coupled fluid-solid system also support a variety of interfacial waves that can propagate much more slowly than the elastic or acoustic speeds (Ferrazzini & Aki 1987). These “crack waves”, as they have been called, are related to Stoneley waves, and persist even when the elastic and acoustic wavespeeds are made infinitely large in comparison to the crack wavespeed. In fact, in that limit, it becomes clear that the crack waves are simply incompressible sloshing modes of the fluid in the channel, as permitted by variations in its thickness and the restoring forces exerted by the elastic walls (see Appendix A). In other words, the crack modes are analogous to the seiches of shallow fluid layers (with gravity playing the same role as the elastic forces), as encountered in harbours, lakes and a variety of other problems in hydraulic engineering. Connections between possible

mechanisms for volcanic tremor and hydraulic transients were recognised already by Ferrick, Qamar & St. Lawrence (1982).

The relatively slow speeds of standing crack waves make them attractive ingredients in the resonance mechanism. Indeed Chouet (1986, 1988) showed that synthetic seismograms generated by such modes of a fluid-filled tabular crack are remarkably similar to some seismograms from volcanoes. Nevertheless, the trigger of the resonance is often neither identified nor specified. There are many plausible origins for fluid pressure transients that could drive resonance impulsively and thereby explain LP events (*e.g.* Konstantinou 2002) but the source of energy driving tremor must be sustained for minutes or much longer.

An alternative perspective presented by Julian (1994) involves a fluid moving through a channel interacting with its deformable rock walls. Flow-induced oscillations arise in many areas of engineering and science and explain phenomena as diverse as the flapping of flags, the sounds of some musical instruments, and noise generation by flow in blood vessels and lung passageways (*e.g.* Backus 1963, Grotberg & Jensen 2004, Pedley 1980). Julian (1994) proposed that a similar instability could be a source mechanism for tremor and LP events at active volcanoes. The flow-induced oscillations could provide the triggering pressure fluctuations to drive resonance with a standing crack wave, but they may also generate harmonic (and non-harmonic) seismic signals by themselves. The mechanism is promising for tremor because the excitation lasts as long as flow is sufficiently fast, and can explain observations of nonlinear phenomena such as period doubling and amplitude-dependent frequency (Julian 1994, 2000; Konstantinou & Schlindwein 2002).

To explore the mechanism, Julian (2004) constructed a “lumped-parameter

model” in which the channel opened and closed uniformly along its length and the rocks were represented by masses on springs with dashpots. Balmforth *et al.* (2005) elaborated further on Julian’s ideas and developed a two-dimensional model coupling semi-infinite elastic blocks with a viscous incompressible channel flow to assess whether hydrodynamic instabilities could arise under volcanological conditions. Here we review and build upon the work of Julian (1994, 2000) and Balmforth *et al.* (2005). More specifically, we consider how flow-induced oscillations might arise in the coupled fluid-solid system illustrated in Figure 1. The geometry consists of two reservoirs that are connected by a relatively narrow channel and maintained at different pressures so that fluid is driven through the channel. For most of the source mechanisms we assess, the details of the reservoirs are not important, and all the action takes place in the flow through the channel, which is relatively vigorous owing to the narrowness of that conduit.

We consider three specific types of flow-induced oscillations: hydrodynamic flow instabilities, flow-destabilized standing waves set up on the channel walls, and unstable normal modes ringing in one of the fluid reservoirs. The hydrodynamic instabilities are analogous to what fluid dynamicists call roll waves (*e.g.* Balmforth & Mandre 2004), and exist when elastic and acoustic wave speeds are infinite. Normal modes of elastic origin that are localized in the channel walls can be destabilized by the flow in a manner similar to the mechanism behind the operation of the vocal chords (Ishizaka & Flanagan 1972). Normal modes in one of the reservoirs can also be made unstable *via* coupling to the channel flow; in this case, the mechanism has many common points with the operation of musical instruments like the clarinet (*cf.* Lesage *et al.* 2006). For each, we summarize the physics involved and determine a criteria for instability on physical and dimensional

grounds. With these results, as well as consideration of the factors that set oscillation frequency, we evaluate the feasibility of them generating low frequency volcano seismicity.

Hydrodynamic flow instabilities

Hydrodynamic flow instabilities in channels need not be generated by fluid interactions with a moving wall. For example in high Reynolds number flow, shear instability can occur in the wake of an irregularity in the channel. The resulting eddy shedding has been suggested as a source of flow transients that could trigger low frequency volcanic resonance (Hellweg 2000). However, because this mechanism requires high Reynolds number flow, it has limited volcanic application. For flow through a deformable channel, there are instabilities at lower Reynolds numbers that are mathematically similar to the roll waves which develop on thin sheets of water flowing down slopes (*e.g.* Balmforth & Mandre 2004). These waves are shock-like flow disturbances with phase speeds similar to the background fluid speed. Analogous instabilities occur in blood flow through deformable veins (Pedley 1980; Brooke, Falle & Pedley 1999) and in slug formation in bubbly two-phase flow (Woods *et al.* 2000). The essential ingredients for roll waves include a force driving flow, viscous or turbulent drag, and a restoring force that flattens disturbances in the free surface (such as gravity, surface tension or, in the volcanic context, the rock elasticity).

Balmforth *et al.* (2005) examined theoretically the generation of roll waves for fluid flow through a thin channel with elastic walls. They treated the fluid as incompressible and viscous, and the walls as semi-infinite linear elastic solids. Generally, magmatic fluids flow much slower than shear

and compressional waves in rocks and it is reasonable to take the limit of infinite elastic wave speeds. Assuming periodic inlet-outlet flow conditions, Balmforth *et al.* found that the roll wave instability requires a finite critical flow speed ($U_{crit\ roll}$) given by

$$U_{crit\ roll} \simeq \beta \sqrt{\frac{\rho_s}{\rho_f}} \epsilon, \quad (1)$$

where β is the shear wave speed in the rock, ρ_s/ρ_f the rock to fluid density ratio, and ϵ is the channel aspect ratio (thickness/length = H/L) with $\epsilon \ll 1$.

This criterion can also be arrived at by simple dimensional arguments. Roll waves are characterized by timescale L/U , where L is the length of the crack and U is the characteristic flow speed. The pressure from the elastic solid due to a displacement, ξ , of the wall is of order $\mu\xi/L$, where μ is the shear modulus of the solid (*i.e.*, Hooke's law). The elastic force induces fluid acceleration and advection of order Uv/L , where v is the perturbation in flow speed. Moreover, conservation of mass demands that Hv be order $U\xi$. Thus, balance is achieved when $\mu\xi/(\rho_f L^2) \sim Uv/L \sim U^2\xi/(HL)$. Rearranging and substituting $\beta = \sqrt{\mu/\rho_s}$ gives the condition of Equation (1).

Note that the presence of the elastic wavespeed in the expression for $U_{crit\ roll}$ is misleading, as there are no elastic waves in this problem; β appears because it also characterizes the restoring force from the elastic walls. In fact, the instability condition does contain a wavespeed, but it is not elastic: for a thin channel of fluid with an elastic wall, waves of thickness variation exist with the wavespeed, $\sqrt{\mu k H / \rho_f} \equiv \beta \sqrt{k H \rho_s / \rho_f}$, where $k \sim L^{-1}$ is the wavenumber. This wavespeed is the limit of the dispersion relation of Ferrazzini & Aki (1987) when the elastic and acoustic waves are relatively large (see Appendix A). In other words, $U_{crit\ roll}$ is the speed of travelling crack waves.

The critical condition implies that roll waves are destabilized by fast flow of dense fluid through long, thin channels. The limitations of roll wave instabilities as a source of volcanic tremor are illustrated in figure (2) which shows $U_{crit\ roll}$ versus ϵ at several values of ρ_f for typical rock properties of $\beta = 1$ km/s and $\rho_s = 2500$ kg/m³. Aspect ratios of magma dykes are usually 10^{-3} to 10^{-2} , and even for a magma with density as high as 3000 kg/m³, sustained flow exceeding 10 m/s is required for tremor by roll waves. Such fast flow rates are problematic given constraints on the size of the dyke from the frequencies, f , of volcanic tremor. Because the wavespeed is order U , f is order (U/L) , where U is the average fluid speed in the basic flow. Generally $f \sim 1$ Hz, which for flow at 20 m/s and $\epsilon = 10^{-3}$ implies a dyke with $L \sim 20$ m and $H \sim 2$ cm (point A on Fig.2). Even flow of a low viscosity magma with $\eta=10$ Pa s through a dyke of these dimensions requires pressure gradients of order 10^7 Pa/m to overcome typical viscous drag. The situation is improved for very long period tremor (*e.g.* 0.1 Hz), which is occasionally observed at volcanoes (*e.g.* Kawakatsu *et al.* 1994) because it allows an order of magnitude larger dyke and thus a substantial decrease in viscous drag. However even for low viscosity basalt the possibility of generating tremor by roll waves is marginal and it is impossible for more viscous (*i.e.* crystal bearing or more silicic composition) magmas to flow sufficiently fast in thin dykes.

The least viscous fluids at volcanoes are gases, but roll-wave development in gas-filled channels is impeded by the low densities (Eq. 1). Despite the small aspect ratios of hydrofractures (typically $10^{-5} < \epsilon < 10^{-4}$), for gas with $\rho_f=1$ kg/m³, roll-wave destabilization requires fluid speeds in excess of 100 m/s (point B on Fig.2) through cracks hundreds of meters long (for $f \sim 1$ Hz). There are, however, fluids at volcanoes of both intermediate den-

sity and viscosity (compared to magma and gases at atmospheric pressure) such as liquid or supercritical H₂O or CO₂-rich fluids, or gases with substantial fractions of suspended rock or magma fragments. The best candidates for roll waves in volcanoes are hot, high pressure H₂O- and CO₂-rich fluids, which have low kinematic viscosities (η/ρ_f). For example H₂O at 500°C and 50MPa has $\rho_f \sim 300 \text{ kg/m}^3$ and $\eta \sim 4 \times 10^{-5} \text{ Pas}$ (Wagner & Overhoff 2006). With such fluids, roll waves of $f \sim 1 \text{ Hz}$ could be generated with reasonable pressure gradients and fracture geometries but still require that high flow speeds of order 10 m/s be sustained for the duration of tremor (*e.g.* point C on Fig.2).

To this point we have assumed typical rock properties of $\beta = 1 \text{ km/s}$ and $\rho_s = 2500 \text{ kg/m}^3$. The flow speeds required to generate roll waves are decreased for porous rocks (reduced ρ_s), partially molten or fluid saturated rocks (reduced β). Also low oscillation frequencies ($< 1\text{Hz}$ as assumed in Fig.2) increase the range of feasible fluid viscosities because longer time scales permit larger channels which in turn reduce viscous drag. However, we still conclude that roll waves require extreme natural conditions and do not provide an explanation for most volcanic tremor.

To make matters worse, a major shortcoming of the Balmforth *et al.* (2005) analysis, on which the above discussion is based, is that the channel has periodic inlet-outlet boundary conditions. This allows roll waves to grow continually as they cycle repeatedly through the domain. In a finite channel, perturbations might be flushed out the end before roll waves have time to develop. One way to characterize the flushing action of the basic flow is in terms of the notion of “convective” and “absolute” instability. Convective instabilities grow exponentially as one moves with the disturbance (until nonlinearity is important), or equivalently if the domain is periodic. At

any given fixed position in a non-periodic channel, however, the disturbance only grows as the instability propagates towards the observer, but is then completely advected past and thereafter decays; *i.e.* it becomes flushed out of the system and can only be sustained if continually fed by external perturbations upstream. By contrast, an absolute instability is one that grows exponentially even at a fixed position; it is impossible for flow to sweep out this instability which amplifies at every point in the channel until quenched by nonlinearity.

Further analysis of the linear stability problem using a method attributed to Briggs (1964), numerical computations with idealized models, and laboratory experiments in shallow water (Liu and Gollub 1993; Mandre 2006) all suggest that roll waves are convective instabilities. We illustrate the essential aspects of the problem in Figure 3, which show numerical solutions of nonlinear roll waves in a model of flow down an elastic-walled channel. Details of the equations of motion and boundary conditions involved in the calculations are relegated to Appendix B. The first computation shown in Figure 3a presents results for a periodic channel, and waves that reach the end of the channel (*e.g.* at $t \sim 100$) reappear at the start of the channel and continue to grow with time. This is in contrast to the computations for a finite channel (Figure 3b,c). Figure 3b is an initial-value problem beginning with random perturbations about the equilibrium flow. Those perturbations seed the growth of roll waves, which subsequently hit the lower boundary and disappear. Perturbations that begin near the outlet barely grow before being flushed out the end; perturbations initially near the inlet do grow into roll waves but when they are flushed out at $t \sim 175$, the roll-wave transient is over. The third computation (c) shows an example in which the initial state is the equilibrium flow but it is continually and randomly perturbed at

the inlet. The perturbations at the boundary now feed the convective roll waves to generate an unsteady flow downstream. How big the roll waves grow depends on the initial level of excitation, the length of the channel and the roll wave growth rate.

LP events could resemble roll wave transients (Fig. 3b), but to generate tremor via roll wave instabilities, there must be a continuous source of agitation at the inlet (Fig. 3c; *i.e.* a trigger for the trigger). Such agitation would be present in most physical systems but we further need the channel to be long enough that the roll waves seeded by the noise amplify sufficiently that they become recognizable nonlinear structures. At the very least, this would require long channels and even higher flow speeds than $U_{crit\ roll}$. Taken together, the instability condition of eq (1) and the lack of an absolute instability lead us to conclude that roll waves could rarely be a source of volcanic tremor.

Elastic normal modes in the channel walls

Much as in Julian's (1994) lumped-parameter formulation, simple models of the vocal chords combine a finite, spatially uniform channel with elastically sprung walls (Ishizaka & Flanagan 1972). The fluid flow destabilizes the oscillations of the walls to generate sound, and the frequencies that become excited are closely connected to the natural oscillation frequency of the springs. Our idealization of the problem shown in Figure 1 can have analogous instabilities if elastic normal modes can somehow be set up in the channel walls which play the role of the springs.

Normal modes are easily set up in finite elastic blocks because standing waves are established in their limited geometry, and their eigenfrequencies

are dictated by the elastic wavespeeds and the block dimensions. In a semi-infinite elastic block, on the other hand, the compressional and shear waves are unable to form a normal mode because they propagate off to infinity and are never reflected back to generate a standing wave. However, the interface also introduces localized Rayleigh waves that can set up standing waves on the channel walls if there is sufficient reflection either from the ends or sides of the channel. This leads to elastic “channel modes” with frequencies determined by the Rayleigh wave speed and the length, L , or width, W , of the channel.

For either configuration, the elastic normal modes can be destabilized by fluid flow, as in the vocal chords, if that flow is sufficiently strong. The precise criterion for instability can be established *via* linear stability theory, as for roll waves, and depends sensitively on the boundary conditions at the flow inlet and outlet (Mandre 2006). Simple estimates for convective instability, which ignores those conditions indicate that the elastic normal modes become unstable when

$$U > U_{crit\ wall} \sim fL,$$

where f is the modal frequency. The dimensional argument behind this result is that the flow destabilizes the mode when the flow time down the channel L/U becomes of the same order as the period of the mode, f^{-1} . Although a comparably simple absolute instability criterion is more difficult to determine, the analysis indicates that destabilized elastic modes have an absolute nature.

Destabilized elastic modes can be readily observed in laboratory experiments of gas flow between a rigid plate and a latex membrane, or through a thin channel cut through a block of gelatine. In either case, the elastic solid begins to ring persistently and harmonically once the flow rate is turned up

beyond some threshold, in line with the preceding arguments (see Figure 4). The fact that oscillations are connected to elastic normal modes is easily verified by checking that the frequency depends linearly on the dimensions of the elastic body (*cf.* Figure 4) and also changes with its properties (*e.g.*, gelatine concentration or membrane tension), but is insensitive to flow speed and fluid density. Note that the threshold in flow speed in the experiment of Figure 4b is roughly 6 m/sec, whereas the mode frequency is about 300 Hz and the channel length is 8cm, which is in agreement with the order of magnitude estimate of $U_{crit\ wall}$.

The unsteady flow through the air channels of both experiments generates audible acoustic signals that can be used to characterize the normal-mode dynamics. Spectra for a number of gelatine experiments are shown in Figure 5. Just beyond the onset of instability, the oscillations are periodic, although the spectrum contains a rich array of harmonics (Figure 5b), as in measurements of volcanic tremor (note that the recording device artificially filters power from the low frequencies, shifting the power maxima to higher frequency). As one increases flow rate, the oscillations become more nonlinear, and phenomena such as frequency gliding and period doubling occur, sometimes even during one experiment (see Figure 5c, which shows period doubling). At the highest flow rates, the periodicity of the signals breaks down as the sides of the channel oscillate so violently that they “slap” together intermittently. These wall collisions destroy the coherence of the elastic mode and generate large amounts of high-frequency noise (Figure 5d).

Note that, because the modal frequency is order β/Δ , where Δ is the dimension of the block along which the standing waves are set up,

$$U_{crit\ wall} \sim \beta \frac{L}{\Delta}$$

(for rock, the compressional, shear and Rayleigh waves all generally travel at roughly comparable speeds). Thus, if the critical flow speed is to be much lower than the elastic wavespeed, the block dimension, Δ , should be much less than the length of the channel. For semi-infinite blocks, this can only be achieved if the channel is much wider than it is long ($W \gg L$), and the elastic mode is composed of lateral, standing Rayleigh waves. (This requirement resonates with one of Julian's (1994) assumptions.) The gelatine block experiment contrasts sharply with this geometrical constraint because shear wave speeds in this material are order m/s, speeds that are easily surpassed by the airflow.

Clarinet modes

For both roll waves and elastic channel modes, the frequency of flow-induced oscillations is set by the dimensions of the channel and the wavespeed within it. Another possibility is that the oscillation timescale is set by the magmatic plumbing system. That is, the channel acts like a clarinet reed that excites and interacts with standing waves in an adjacent reservoir. In that musical instrument the sound produced is not simply a result of a resonance between the frequencies generated by the oscillating reed and a mode in the neighbouring air column; by itself the reed vibrates at much higher frequencies. Instead, it is the coupling between the flow in the reed and the feedback from the resonating air column at its outflow that produces the sound as an intrinsic instability (e.g. Backus 1963).

By combining a shallow channel flow theory like that of Appendix B with a compressible fluid column to represent the reservoir, one is again able to formulate a simple mathematical model to explore the feasibility of

this mechanism in the volcanic setting. A convective stability analysis with the model then implies that the threshold for instability takes the form,

$$U_{crit \text{ reservoir mode}} \sim \frac{c_{acoustic}L}{D}, \quad (2)$$

where $c_{acoustic}$ is the sound speed in the fluid and D is the dimension of the reservoir. The oscillation frequency for reservoir modes is $c_{acoustic}/D$, so the instability condition again compares the flow speed with a wavespeed, including a relevant geometrical factor.

Once more, there is a justification for this condition on physical and dimensional grounds: A pressure perturbation at the end of the channel will be transmitted by acoustic waves through the reservoir and return to the channel after a time of order $\sim D/c_{acoustic}$. For $L \ll D$ the pressure perturbation at the channel outlet will affect flow at the inlet essentially instantaneously, so to couple effectively the channel and reservoir and build the required feedback, one must match the timescale for flow through the channel, $\sim L/U$, with the timescale for acoustic waves to traverse the reservoir, $\sim D/c_{acoustic}$. Note the channel could be upstream or downstream of the reservoir. In practice, viscous forces and incomplete reflections will cause damping of the reservoir modes, and must be overcome by the fluid driving at the reed in order to set up and sustain tremor.

Therefore, to excite oscillations, the flow must exceed a fraction of $c_{acoustic}$. For fluids in volcanoes, $c_{acoustic}$ varies from less than 10^2 m/s in magma with 30-70% bubbles to greater than 10^3 m/s in bubble-free magma (H_2O and CO_2 -rich fluids having intermediate sound speeds; Morrissey & Chouet 2001). Although $c_{acoustic}$ is fast compared to flow speeds, L/D can be extremely small such that reasonable flow speeds could destabilize the reservoir acoustic mode. Nevertheless the reservoir length must still be well over 100m in order for the modal frequency to match typical tremor.

Discussion

In this article, we have reviewed three mechanisms by which oscillations can be generated by flow down an elastic channel: hydrodynamic instabilities (roll waves), destabilized elastic wall modes, and unstable normal modes in an adjacent reservoir. We have already pointed out that roll waves are unlikely in the geological context because they require relatively high flow speeds and may require seeding by external perturbations in long channels so that they are not flushed out. Note that these disturbances are unstable waves of thickness variation in the channel, propagating in the direction of flow. As such, they are equivalent to travelling crack waves, modified by the mean flow. The (convective) instability criterion for these disturbances is equivalent to the requirement that the flow is faster than those travelling waves.

Elastic modes in the channel walls are destabilized by the flow according to a similar stability criterion, $U > \beta(L/\Delta)$, with Δ being the dimension of the elastic body along which the elastic standing waves are set up. Such flow speeds may be achieved in the geological context if the channel is much wider than it is long. However, the mode frequency f is of order β/Δ , and for the $O(1)$ Hz frequencies characteristic of tremor, the relevant dimension of the elastic body must then be of order a kilometer and is implausibly large (this is the same argument that dismisses any resonant *elastic* body as the origin of tremor, and motivates the introduction of a fluid-filled channel). Equivalently, if the elastic body has a realistic length, then there is a problem with its natural timescale. This is unfortunate given the relative ease with which the elastic modes can be destabilized and their nonlinear properties, which resemble tremor observations.

The lumped-parameter model for volcanic tremor put forward by Julian

(1994) does not capture propagating disturbances like roll waves, and is much like the models of the vocal chords (or blood vessels, Pedley 1980) in which elastic modes are destabilized. Indeed, his tremor frequencies are partly set by the natural oscillation frequency of the wall springs. Julian is also careful to draw a distinction between his model and resonant crack modes. Thus, one might, at first sight, think that the instabilities in his model may be destabilized elastic modes, in which case there is a timescale problem. However, Julian’s model also incorporates unsteady fluid motions which affect the frequency of fluid-induced oscillations. Julian refers to the effect as “added mass”, giving the impression that his modes are fluid-modified elastic modes. In fact, those unsteady fluid motions correspond to thickness variations of the channel, and provide a natural oscillation even if the inertia of the springs is discarded (removing the normal mode in the elastic walls). In other words, Julian’s model also contains a type of crack mode. And from his prescription of the restoring force, it is clear that these modes are standing crack waves across the width of the channel. Altogether, this suggests that the timescale problem of destabilized channel modes might be avoided if these modes are not of elastic origin, but are hydrodynamic crack, or “sloshing” modes, like seiches.

Channel modes are not required whatsoever in the clarinet-type mechanism, which sets up the flow-destabilized oscillation in an adjacent reservoir. In the musical instrument, the reservoir mode is of acoustic origin, and so the sound speed and reservoir length set the timescale. Because the sound speed can be an order of magnitude smaller than the elastic wave speed in rock, acoustic reservoir modes have less of a timescale problem than elastic channel modes. One still remains, however, because some magmas can have quite high sound speeds. Moreover, acoustic waves could be strongly

damped in a viscous fluid reservoir, which raises the flow speed required to drive instability. All these problems might again be avoided again if the reservoir mode is not actually acoustic, but a crack or sloshing mode.

The theory for destabilized sloshing modes either in the channel or a reservoir remains to be worked out. Our expectation is that the critical flow speeds required to drive oscillations are related to crack wave speeds together with a geometrical factor, as in the three mechanisms discussed here. If this is borne out, and since the relatively low crack wave speed could resolve the timescale problem, such modes might provide the most plausible explanation of long-period volcanic seismicity.

Given that the mechanism and mode type might eventually be the same for both unstable channel and reservoir modes, the distinction between them boils down chiefly to one of geometry, and one wonders how one might choose between them seismologically. In this regard, a key geometrical detail is source location within the resonant body: the source for the channel modes occurs throughout its width, although one might imagine that flow speeds are greatest, and therefore instability strongest, closest to the midline. By contrast, the reservoir modes are always driven from one end. Along the lines suggested by Chouet (1988), one might then be able to use seismic signature to tell the difference between reservoir and channel modes.

Finally, it is intriguing that there are observations of non-volcanic tremor in singing icebergs (Müller *et al.* 2005) and hydrocarbon reservoirs (Dangel *et al.* 2003). These other contexts can be more accessible or provide other constraints and thereby offer critical tests of the ideas and theory.

A Slow crack waves

If we neglect viscous drag, linear motions of two-dimensional incompressible fluid in a thin, uniform channel can be described by the shallow-water-like model (*cf.* Appendix B),

$$\eta_t + H u_x = 0, \quad u_t = -\frac{1}{\rho_f} p_x$$

where η is the variation in channel thickness, and u and p are the associated flow speed and pressure perturbations. Assuming wave-like disturbances of the form, $\exp ik(x - ct)$, where k is wavenumber and c is wavespeed, we find

$$c^2 \eta = \frac{H}{\rho_f} p.$$

The pressure is related to the wall displacement according to the mechanics of the elastic wall. For semi-infinite blocks with elastic wavespeed much greater than c ,

$$p = \frac{k\mu\eta}{2(1 - \sigma)},$$

where σ is Poisson's ratio. Waves therefore travel with the phase speed,

$$c = \sqrt{\frac{\mu k H}{2\rho_f(1 - \sigma)}}.$$

This result is identical to the limiting form of Ferrazzini & Aki's dispersion relation for symmetrical crack modes. Note that Chouet's "crack stiffness" (which uses the ratio of solid and fluid bulk moduli) is not the natural parameter to describe these slow crack waves in this limit because the fluid motions are incompressible.

B Details of mathematical model

When the fluid channel is much thinner than it is wide, fluid variations across the channel are much greater than variations in the flow directions

and along the slot. Taking a “thin-channel” approximation (*e.g.* Balmforth *et al.* 2005), our fluid model consists of slot-averaged equations for the local thickness, $h(x, t)$, and speed, $u(x, t)$, which represent conservation of mass and momentum along the slot (the x -direction):

$$h_t + (uh)_x = 0, \quad u_t + uu_x = \frac{\Delta}{h^2}(U - u) - \frac{p_x}{\rho_f}, \quad (3)$$

Here, Δ is a viscous drag coefficient, U is the mean flow speed and $p(x, t)$ is the pressure perturbation induced in the fluid stemming from the motion of the wall. The model assumes $p = \Gamma(h - H)$, where Γ is a constant, and H is the equilibrium channel thickness. These choices correspond to the wall responding like a simple elastic foundation (a mattress) and flow resistance stemming from an approximation of laminar viscous drag. In the Figure 3 we choose units such that $\Gamma/\rho_f = 1/5$, $\Delta = 1/5$, $U = H = 1$ and $L = 200$.

For boundary conditions we use either periodic conditions on u and h (Figure 3a), or fixed flux (hu) and pressure (equivalently h) at the inlet, and $(hu)_x = 0$ at the outlet (Figure 3b,c).

References

- [1] Backus, J. 1963. Small-vibration theory of the clarinet. *Journal of the Acoustical Society of America*, **35**, 305–313.
- [2] Balmforth, N. J. & Mandre, S. 2004. Dynamics of roll waves. *Journal of Fluid Mechanics*, **514**, 1–33.
- [3] Balmforth, N. J., Craster, R. V. & Rust, A. C. 2005. Instability in flow through elastic conduits and volcanic tremor. *Journal of Fluid Mechanics*, **527**, 353–377.

- [4] Briggs, R. J. 1964. *Electron-stream interaction with plasmas*. MIT Press (Cambridge, MA).
- [5] Brook, B. S., Pedley, T. J. & Falle, S. A. 1999. Numerical solutions for unsteady gravity-driven flows in collapsible tubes: evolution and roll-wave instability of a steady state. *Journal of Fluid Mechanics*, **396**, 223–256.
- [6] Chouet, B. 1986. Dynamics of a fluid-driven crack in 3 dimensions by the finite-difference method. *Journal of Geophysical Research*, **91**, 13967-13992.
- [7] Chouet, B. 1985. Excitation of a buried magma pipe - a seismic source model for volcanic tremor. *Journal of Geophysical Research*, **90**, 1881-1893.
- [8] Chouet, B. 1988. Resonance of a fluid-driven crack - radiation properties and implications for the source of long-period events and harmonic tremor. *J. Geophys. Res.*, **93**, 4375-4400.
- [9] Chouet, B. 1996. Long-period volcano seismicity: its source and use in eruption forecasting *Nature*, **380**, 309-316.
- [10] Chouet, B. 2003. Volcano seismology. *Pure and Applied Geophysics*, **160**, 739–788.
- [11] Dangel, S., Schaepman, M. E., Stoll, E. P., Carniel, R., Barzandji, O., Rode, E.-D. & Singer, J. M. 2003. Phenomenology of tremor-like signals observed over hydrocarbon reservoirs. *Journal of Volcanology and Geothermal Research*, **128**, 135-158.

- [12] Ferrazzini, V. & Aki, K. 1987. Slow waves trapped in a fluid-filled infinite crack. *Journal of Geophysical Research*, **92**, 9215-9223.
- [13] Ferrick, M. G., Qamar, A. & St. Lawrence, W. F. 1982. Source mechanism of volcanic tremor. *Journal of Geophysical Research*, **87**, 8675-8683.
- [14] Grotberg, J. B. & Jensen, O. E. 2004. Biofluid mechanics in flexible tubes. *Annual Review of Fluid Mechanics*, **36**, 121-147.
- [15] Hagerty, M. T., Schwartz, S. Y., Garces, M. A. & Protti, M. 2000. Analysis of seismic and acoustic observations at Arenal volcano, Costa Rica, 1995-1997. *Journal of Volcanology and Geothermal Research*, **101**, 27-65.
- [16] Hellweg, M. 2000. Physical models for the source of Lascar's harmonic tremor. *Journal of Volcanology and Geothermal Research*, **101**, 183-198.
- [17] Ishizaka, K. & Flanagan J. L. 1972. Synthesis of voiced sounds from a two-mass model of the vocal chords. *Bell Systems Technology Journal*, **51**, 1233.
- [18] Julian, B. R. 1994. Volcanic tremor: nonlinear excitation by fluid flow. *Journal of Geophysical Research*, **99**, 11859-877.
- [19] Julian, B. R. 2000. Period doubling and other nonlinear phenomena in volcanic earthquakes and tremor. *Journal of Volcanology and Geothermal Research*, **101**, 19-26.
- [20] Kawakatsu, H. Ohminato, T. & Ito, H. 1994. 10s-period volcanic

- tremors observed over a wide area in southwestern Japan. *Geophysical Research Letters*, **21**, 1963–1966.
- [21] Konstantinou, K. I. 2002. Deterministic non-linear source processes of volcanic tremor signals accompanying the 1996 Vatnajökull eruption, central Iceland. *Geophysical Journal International*. **148**, 663–675.
- [22] Konstantinou, K. I. & Schlindwein, V. 2002. Nature, wavefield properties and source mechanism of volcanic tremor: a review. *Journal of Volcanology and Geothermal Research*, **119**, 161–187.
- [23] Lesage, P., Mora, M. M., Alvarado, G. E., Pacheco, J. & Metaxian, J.-P. 2006. Complex behaviour and source model of the tremor at Arenal volcano, Costa Rica. *Journal of Volcanology and Geothermal Research*, **157**, 49-59.
- [24] Liu, J., Paul, J. D. & Gollub, J. P. 1993. Measurements of the primary instabilities of film flows. *Journal of Fluid Mechanics*, **250**, 69-101.
- [25] Mandre, S. 2006. *Two studies in hydrodynamic stability. Interfacial instabilities and applications of bounding theory*. PhD thesis, University of British Columbia.
- [26] McIntyre, M., Schumacher, R.T. & Woodhouse, J. 1983. On the oscillations of musical instruments. *Journal of the Acoustical Society of America*, **74**, 1325-1345.
- [27] McNutt, S. R. 2005. Volcanic Seismology. *Annual Review of Earth and Planetary Sciences*, **33**, 461-491.
- [28] Morrissey, M. M. & Chouet, B. A. 2001. Trends in long-period seismic-

- ity related to magmatic fluid compositions. *Journal of Volcanology and Geothermal Research* **108**, 265–281.
- [29] Müller, C., Schlindwein, V., Eckstaller, A., & Miller, H. 2005. Singing Icebergs. *Science* **310**, 1299.
- [30] Pedley, T. J. 1980. *Fluid mechanics of large blood vessels*. Cambridge University Press.
- [31] Wagner, W. & Overhoff, U. 2006. *Extended IAPWS-IF97 Steam Tables*. Springer-Verlag, Berlin, Heidelberg.
- [32] Woods, B. D., Hurlburt, E. T. & Hanratty, T. J. 2000. Mechanism of slug formation in downwardly inclined pipes. *International Journal of Multiphase Flow*, **26**, 977-998.

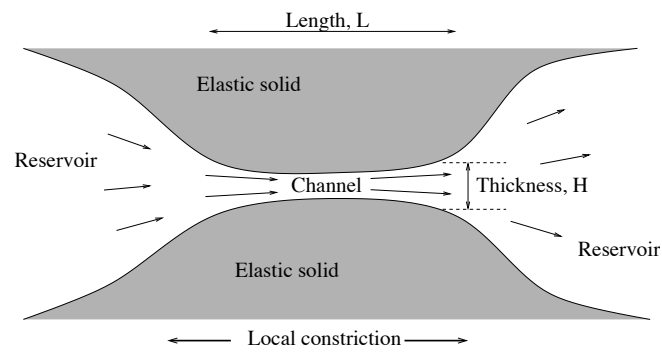


Figure 1: Schematic illustration of a channel between two reservoirs. Flow is driven through the channel by a pressure difference maintained between the reservoirs. The channel is tabular, and its walls deform elastically in response to pressure changes in the fluid.

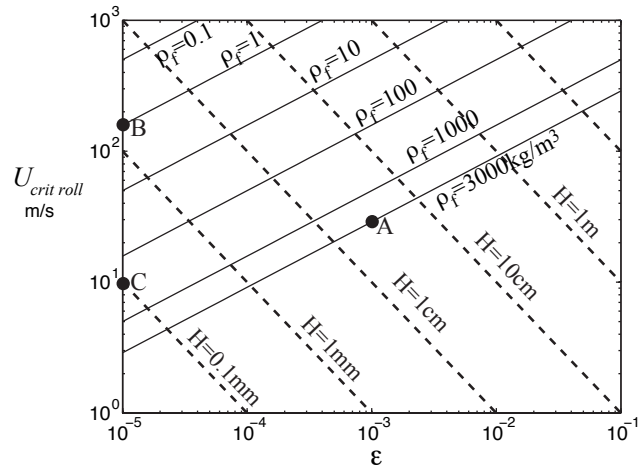


Figure 2: Critical flow speed (from Eq.1) for roll waves versus channel aspect ratio for several fluid densities (solid lines) for constant rock properties of $\beta = 1$ km/s and $\rho_s = 2500$ kg/m³. Dashed lines indicate crack thickness for $f \sim U/L \sim 1$ Hz. Points A,B and C refer to conditions discussed in the text.

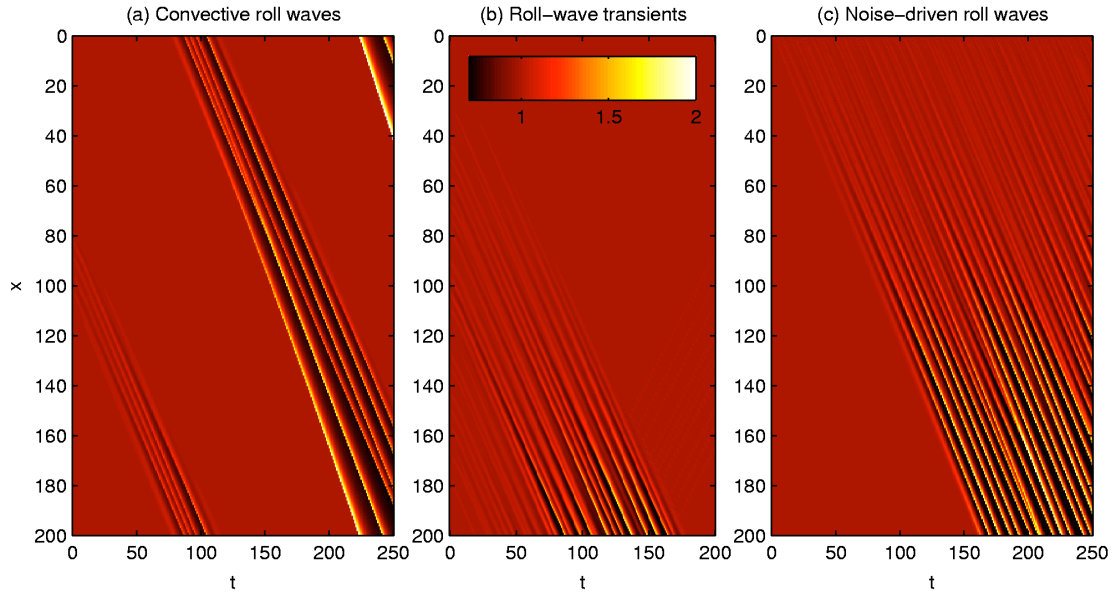


Figure 3: Numerical solutions of the simple two-dimensional flow model described in Appendix B. The three panels show how the local channel thickness h varies with downstream position (x) and time (t). The shading indicates h as shown in the legend in (b), with $h = 1$ corresponding to the unperturbed, equilibrium thickness of the channel. In (a) the domain is periodic and the initial condition consists of random perturbations about the equilibrium flow, concentrated near mid-channel, with a peak-to-peak amplitude of less than 10^{-2} . Panel (b) shows a finite domain with the boundary conditions described in Appendix B. There is a similar, random initial condition to panel (a), but here the perturbations are evenly distributed throughout the channel length. Panel (c) shows a computation in a finite domain with the same boundary conditions as (b), except that roll waves are continually seeded by random noise added to the equilibrium flow at the inlet ($x = 0$) for the entire simulation duration.

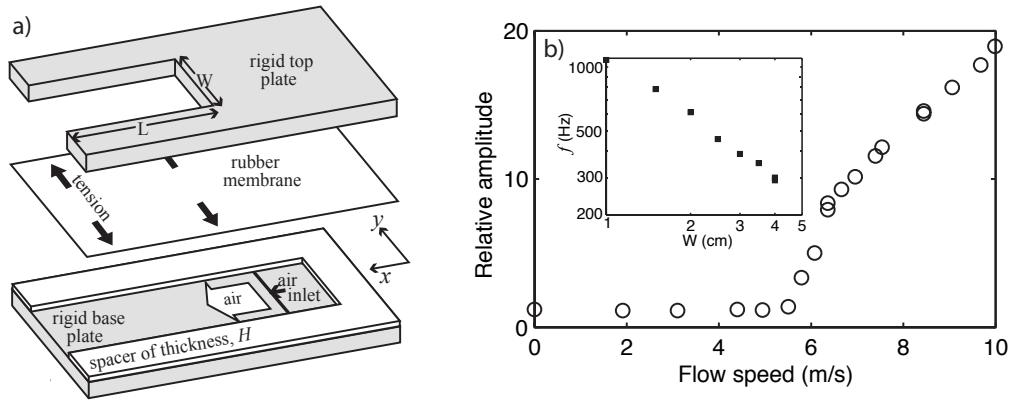


Figure 4: a) The apparatus for experiments of gas flow between an elastic membrane and a rigid plate. The components illustrated were laid on top of each other and clamped together exposing a membrane of size W by L stretched parallel to the y -axis. Compressed air, nitrogen or helium was input from below, flowed in the x direction and exited at the free boundary. b) The amplitude of the sound recorded, relative to ambient levels, versus flow speed for an elastic membrane experiment with $L = 8$ cm, $W = 4$ cm and $H = 0.19$ mm. The critical fluid speed for the onset of elastic oscillations is between 5.5 and 5.8 m/s. The inset shows frequency of oscillations against W for a set of experiments where the membrane tension, L and H were held constant (including data from panel a).

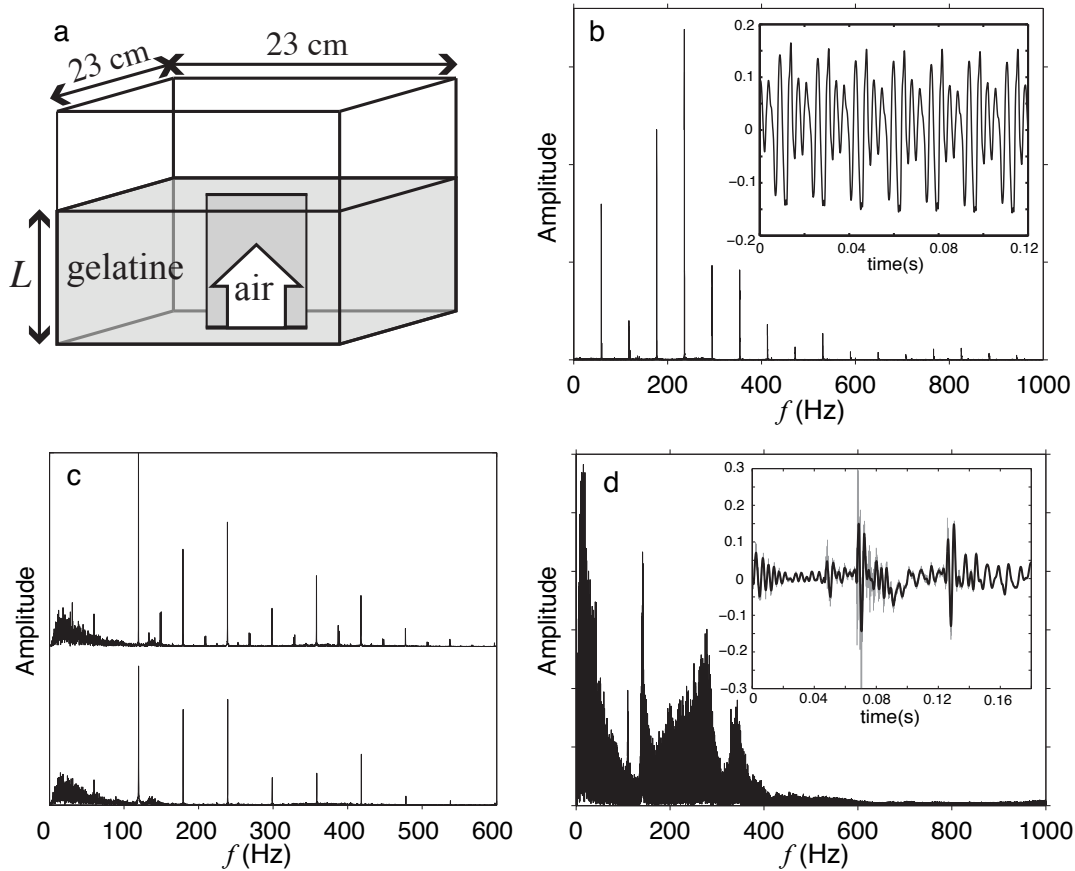


Figure 5: a) The apparatus for gelatin block experiments. Air flows up a vertical slit cut in the block. The length of the slit, L , is the height of the gelatin, which varied from 6 to 12 cm. b) Frequency spectrum and time series (inset) of the audio signal generated by a pressure drop of 1.5 kPa driving air through a 10wt % gelatine block with $L = 6$ cm. The time series is filtered to remove frequencies greater than 1200 Hz. (c) Frequency spectra illustrating period doubling. Each of the spectra shows the frequency content for 10 seconds of the continuous experiment (7.5% wt gelatine, $L = 12$ cm, air pressure drop of 3.6 kPa). (d) Frequency spectrum and time series for a signal generated by 5% wt gelatine block with $L = 12$ cm and an air pressure drop of 2.8 kPa. The unfiltered time series is grey and the low-pass filtered signal (<1200 Hz) is in black. The strongest slapping event is at about 0.7 s.